

# New insights on chemical evolution of galaxies: *XMM-Newton* observations of M82

P. Ranalli\* <sup>a</sup>, L. Origlia<sup>b</sup>, A. Comastri<sup>b</sup> R. Maiolino <sup>c</sup>

<sup>a</sup>Cosmic ray laboratory, RIKEN, 2-1 Hirosawa, Wakoshi, Saitama, 351-0198 Japan

<sup>b</sup>INAF–O.A.Bologna, via C. Ranzani 1, 40127 Bologna, Italy

<sup>c</sup>INAF–O.A.Arcetri, Largo E. Fermi 5, 50125 Firenze, Italy

We report on the ongoing data analysis of a very deep ( $\sim 100$  ks) *XMM-Newton* observation of the starburst galaxy M82. We show some details of data analysis and a few results from spatially-resolved spectroscopy with the EPIC cameras. Since M82 is a bright object with a complex spectrum, the data reduction of such a deep observation has posed many challenges both about the involved astrophysical processes and the available data analysis techniques. Vertical (with respect to the galaxy plane) abundance gradients are discovered. The hints for an under-abundance of Oxygen stemming from our previous study are confirmed. The hot X-ray emitting gas is shown to have a multi-temperature distribution.

## 1. Introduction

The signature of the star formation (SF) history of a galaxy is imprinted in the abundance patterns of its stars and gas. Determining the abundance of key elements released in the interstellar medium (ISM) by stars with different mass progenitors and hence on different time scales, will thus have a strong astrophysical impact in drawing the global picture of galaxy formation and evolution [8]. It also offers the unique chance of directly witnessing the enrichment of the ISM [7]. Metals locked into stars give a picture of the enrichment just prior to the last burst of SF, while the hot gas heated by SNe II explosions and emitting in the X-rays should trace the enrichment by the new generation of stars.

We have started a project to measure the detailed chemical abundances in a sample of starburst galaxies, for which we obtained high resolution infrared (J and H band) spectra with the 3.6 m Italian Telescopio Nazionale Galileo (TNG) and with the ESO VLT, and both proprietary and archival data from the *XMM-Newton* and *Chandra* missions. Our sample comprises M82, NGC253, NGC4449, NGC3256 and the *Antennae*, sampling two orders of magnitude in star formation, as it ranges from the  $0.3 M_{\odot}/\text{yr}$  of NGC4449 to the  $\sim 30 M_{\odot}/\text{yr}$  of the *Antennae* and NGC3256.

Preliminary results for M82 were achieved with the available *XMM-Newton* archival data, and hinted for a confirmation of the expected scenario in which the gaseous component has a higher content of  $\alpha$ -elements than the stellar one, and a similar content of Fe [10]. However, some new issues were posed, since we found a very low abundance of O and Ne with respect to other  $\alpha$ -elements (e.g., O/Mg  $\sim 0.2$ , Ne/Mg  $\sim 0.3$ ) in the hot gas present in the central ( $< \sim 1$  kpc) regions of M82, which could not be satisfactorily explained. For this reason, we were granted a deeper observation of M82. A report on our preliminary analysis appeared in [12]. Some issues concerning the data analysis of complex and well-sampled spectra by standard “black box” tools, such as XSPEC, the Mekal and APEC models, etc. are presented in this contribution. The main paper is currently in preparation.

## 2. EPIC data reduction at the limits of standard tools

M82 is a bright galaxy with an ongoing starburst and a complex spectrum. Thus, the data reduction of such a deep observation (100 ks) has proved difficult and time-consuming, posing many challenges about the involved astrophysical processes and the available software apparatus.

The EPIC data were analysed with the SAS software, version 6.5.0. After screening for background flares, about 73 ks of data were accepted

---

\*JSPS fellow.

for analysis. We began our analysis from the central region of M82, by extracting spectra from a circle with diameter  $1'$  and centred on the coordinates 09:55:51 and +69:40:39. Background spectra were extracted from the blank-sky data files [13] after normalisation to the background levels observed in the M82 data.

The largest emission from hot plasma is found in the centre of M82. However, many point sources are also present in the same region. To choose a model for the point sources, we analysed the spectrum in the 3–8 keV band, and we found that it can be well described by a power law with photon index  $\Gamma = 1.60^{+0.04}_{-0.03}$ . This power law has been always included in the models discussed below regarding the centre of M82. A Fe thermal line is also detected at  $6.66 \pm 0.02$  keV with equivalent width  $\sim 100$  eV.

The abundances for O, Ne, Mg, Si, S, Fe were left free to vary, since these elements have strong lines in the considered wavelength range. Other  $\alpha$ -elements with weaker lines (Na, Al, Ar, Ca), which would not be sufficiently constrained on their own, were bounded together using solar ratios, accordingly to the proximity in their atomic number, e.g Na and Al to Mg, Ar and Ca.

## 2.1. Multi-temperature plasma

In the literature, the gaseous emission is usually modelled with one or two single-temperature components. A ‘warm’ component usually around 0.7–1 keV is almost ubiquitous [11]. A high energy component is also often reported [3,2] in studies based on ASCA or BeppoSAX data, described either as a power-law, or as a thermal spectrum with  $kT \sim 4$ –10 keV. Because of the poor spatial resolution of those satellites it is not clear if this component is really diffuse or rather due to point sources. Thus, some care should be taken in comparing literature results with this paper, since in the following we’ll account for both point sources (via the power law discussed in the previous paragraph) and for hot gas. A ‘cold’ component, around 0.1–0.3 keV, is also found sometimes [4]. In general, the better the quality of data, the larger the number of components required to provide an acceptable fit. Thus, the use of multi-temperature models that allow for a fine control of the DEM, and are also insensitive to the Fe-bias [1], might be preferable but this is hardly feasible, because of demanding requirements in data quality and computing time. The grade of

our M82 observation is sufficiently high to allow for the first time the use of multi-temperature models even in spatially-resolved spectroscopy.

The results of the fit showed that a hot component ( $kT > \sim 5$  keV) is required in order to fit the spectrum. Several versions of the common MEKAL code [9] are present with multi-temperature flavours in the XSPEC distribution (version 11.3.2g), among which the most flexible are `c6vmek1` and `c6pvmk1`. These models parameterise the plasma DEM, i.e. the amount of plasma with a given temperature, with a 6<sup>th</sup> order polynomial, and allow for variable abundances. The difference between them is that `c6pvmk1` restricts the DEM to positive values, while `c6vmek1` also allows negative values: this means that negative amounts of plasma are permitted. Thus we chose to use `c6pvmk1`.

However, these models allow only temperatures with  $kT \leq 7$  keV, causing the best-fit DEM to have a sharp cut, clearly noticeable in Fig. 1 (left panel). Feeling that this limitation was somewhat artificial, we modified the available multi-temperature plasma models by enlarging the allocated energy range, so that the high-temperature part of the DEM could be better sampled. The best fit DEM for both the standard and ‘enlarged’ models are shown in Fig. 1. The improvement in  $\chi^2$  was however not significant, indicating that the DEM sampling was already sufficiently good: as it may be seen in Fig. 1, the high-temperature component is distributed like a rather narrow bell curve, so little difference is found between a single temperature component and the sum of two components with very similar temperatures.

We also checked if the hot component could have a non-thermal origin: since star forming galaxies are known as radio sources, bremsstrahlung emission should in principle arise from the same population of electrons from which the synchrotron emission is originated. Thus we developed a non-thermal bremsstrahlung model for XSPEC. We found that the hot thermal component could not be replaced by a non-thermal one, because of *i*) the fit statistics worsens; *ii*) given the observed X-ray flux from the non-thermal bremsstrahlung component, and hence the required population of free electrons, an unrealistically low galactic magnetic field would be required to account for the observed radio (synchrotron) emission.

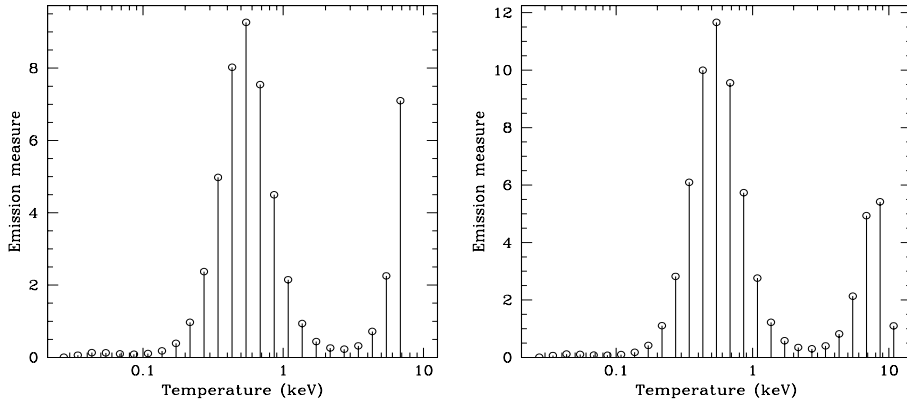


Figure 1. The best fit DEM for the central regions of M82 by using the standard `c6pvmk1` model (left panel) and its enlarged-energy-array version (right panel). The total spectrum is computed by adding several components, one for each sampling point shown here.

## 2.2. Unidentified lines

There seems to be two lines in the data which are not present in the model (see Fig. 2). If the lines are parameterised with Gaussian models, the best fit energies are  $1.22 \pm 0.01$  keV (equivalent width  $\sim 17$  eV) and  $\sim 0.78$  keV (equivalent width  $\sim 20$  eV).

These lines are present through all the spatial extent of the outflow, which is about the central  $10'$  of the MOS and PN chips. By looking at the Chianti line emission database [5] the best candidates for the 1.22 keV line are the Fe XVII line at 1.223 keV or the Ne X line at 1.211 keV, while for the 0.78 keV line the best candidate is the Fe XVIII line at 0.7832 keV. Although *i*) the effective areas in all EPIC cameras in the considered energy range are a smooth function of the wavelength and do not show any feature around the considered wavelengths, and *ii*) no background feature is present near the considered wavelengths (moreover, the count rate of the central region of M82 is about 100 times larger than the background), we believe that these lines might also be instrumental, background or model features, for:

- the 1.22 keV line is flanked at longer wavelengths by an absorption-like feature. A close look to Fig. 2 suggests that a line, if indeed present, should be accompanied by problems in modelling the continuum.
- The 1.22 keV line is not present in the RGS data (Fig. 3), and the other one at 0.78 keV

seems to be present with lesser intensity. However, this might also be due to the RGS counts being  $\sim 1/10$  of the EPIC ones.

- The line intensity is reduced if the APEC model is used in place of Mekal (see below).

To further check whether the presence of the two ‘unidentified lines’ might be related to the details of the spectral model, we fitted the data using the APEC model [14]. Since no multi-temperature APEC model is present in the current XSPEC distribution, we built one based on the Mekal one, with the only difference that the APEC routines are called. Switching from the Mekal- to the APEC-based model improves the fit: for the Mekal one, one gets, considering only the MOS spectra,  $\chi^2 = 1459$  with 889 degrees of freedom (d.o.f.;  $\chi^2 r = 1.64$ ); for the APEC one,  $\chi^2 = 1274$  ( $\chi^2 r = 1.43$ ). A visual inspection of the residuals confirms that the APEC model provides a better representation of the data (Fig. 3). As a technical note, we point out that no significant difference in the value of  $\chi^2$  was obtained for the Mekal model with the `switch` parameter set to “calculate”, as opposed to the default value of “interpolate from a pre-calculated table” (see the XSPEC documentation).

Thus, we decided to treat these lines as non-astrophysical features. A detailed comparison of the calculations from the two considered spectral codes is being performed, and its results are deferred to the main paper in preparation.

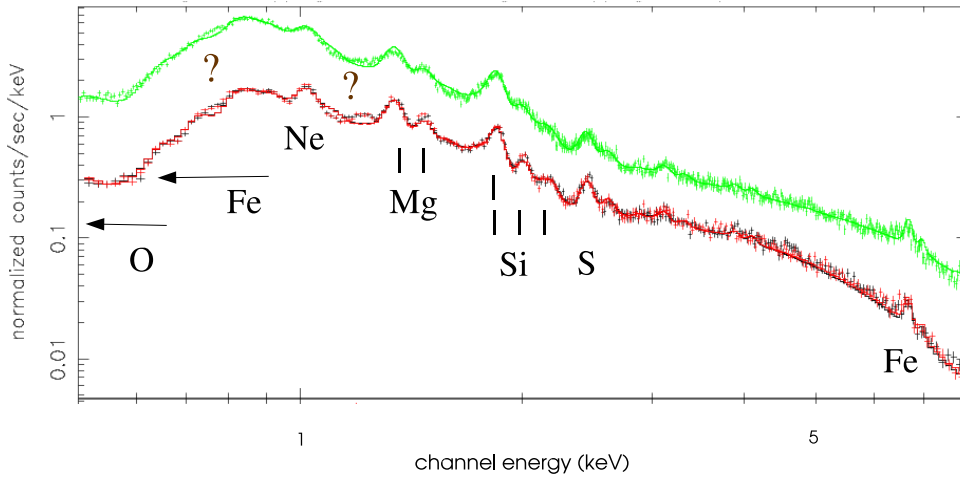


Figure 2. EPIC spectra of the central ( $2'$ ) region of M82. Green points (upper data series): PN. Red and black points (lower data series): MOS. Some of the strongest emission lines are indicated. The arrows below Fe and O show line blends. The position of the two ‘unidentified lines’ is also shown with a question mark.

### 3. RGS data

The RGS spectra for the inner region were extracted with the `rgsproc` tool, considering only events within 90% of the PSF width (i.e.  $\sim 1'$ ) in the cross-dispersion direction. The background spectra were taken from the blank-sky observations using the `rgsbkgmodel` tool. The line width in the RGS data is dominated by the M82 size ( $\sim 2'$ ) so the `rgsxsrc` XSPEC model, which convolves the instrumental line width with the source spatial profile, has been used to account for the source extent. This model needed to be patched to allow the joint fit of grating and CCD data. The spectra are shown in Fig. 3. The best fit parameters from fits to either the joint EPIC-RGS data and RGS data alone are consistent with being a spatially-weighted average of those discussed above (see Fig. 5).

### 4. Spatially resolved spectroscopy

We report here on the preliminary analysis conducted on both the northern and the southern outflows, mainly making use of EPIC. In order to study the different properties of the hot gas as it flows and/or is heated from the central starburst towards the intergalactic space, we divided both outflows in five sub-regions. Each region has a rectangular shape, the larger side being

parallel to the galaxy major axis. The spectra were extracted from the MOS (0.5–8.0 keV) and PN (1.0–9.0 keV) data, and fitted with the same model used for the central region, the only difference being point sources, which in the outflow are sufficiently apart to be excluded when extracting spectra.

The best-fit chemical abundances from EPIC and RGS data are shown in Fig. 5 along with results from our previous paper [10] relative to infrared observations for the central regions. The abundances are scaled according to the Grevesse & Sauval [6] solar composition. No significant changes are found in the temperature of the plasma. Only one region required in its spectrum some absorption in excess of the Galactic value. Our previous finding, that the inner region of M82 is somewhat devoid of the lighter  $\alpha$ -elements, is thus confirmed. Moreover, it is found that all elements are more concentrated in the outflow than in the centre. The centre/outskirt abundance ratio ranges from  $\sim 1/10$  for O to  $\sim 1/3$  for the heavier elements (Mg, Si, S).

In M82 both the hot gas and the stellar phases trace a very similar Fe abundance. Indeed, since Fe is mainly produced by type Ia supernovae (SN), it is expected to be significantly released in the ISM only after a few 100 Myr from the local onset of star formation. At variance,  $\alpha$ -elements

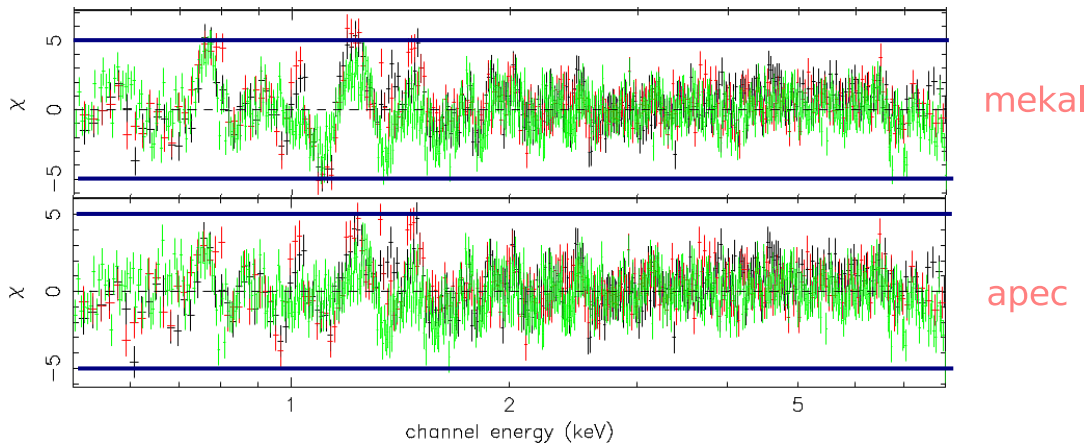


Figure 3. Residuals of EPIC data with different models. The model parameters are best-fit ones and thus are slightly, yet not significantly, different in the two cases. The reduced  $\chi^2$  are 1.64 for Mekal and 1.43 for APEC.

(O, Ne, Mg, Si, S) are predominantly released by type II SN with massive progenitors on much shorter time scales.

The overall  $\alpha$ -elements/Fe enhancement is consistent with a standard chemical evolution scenario only for the heavier elements (Mg, Si, S). The lighter elements (O, Ne) show a different distribution: in the inner regions of the galaxy, the O/Fe and Ne/Fe ratios appear to be too low for this scenario to hold. In fact, the X-ray derived O abundance in the centre is less than the infrared-derived one.

## 5. Conclusions

The analysis of a very deep ( $\sim 100$  ks) observation of the starburst galaxy M82 has opened some new questions, which may be summarised as:

- there is a discrepancy in the oxygen abundance between the hot gas and stars, which goes in the opposite direction with respect to the expectation of chemical evolutionary models;
- strong vertical abundance gradients in some metals have been discovered;
- the X-ray emitting gas has a “multi-temperature” nature.

We have worked out some possibilities for interpreting these results, which will be presented in the forthcoming main paper.

## REFERENCES

1. Buote, D. & Fabian, A.1998, MNRAS, 296, 977
2. Cappi, M., Persic, M., Bassani, L. *et al.* 1999, A&A, 350, 777
3. della Ceca, R., Griffiths, R. & Heckman, T.1997, ApJ, 485, 581
4. della Ceca, R., Griffiths, R., Heckman, T. *et al.* 1999, ApJ, 514, 772
5. Dere, K., Landi, E., Young, P. *et al.* 2001, ApJS, 134, 331
6. Grevesse, N. & Sauval, A.1998, Space Science Reviews, 85, 161
7. Maeder, A. & Conti, P.1994, ARA&A, 32, 227
8. McWilliam, A.1997, ARA&A, 35, 503
9. Mewe, R., Kaastra, J. & Liedahl, D.1995, ApJ, 6,
10. Origlia, L., Ranalli, P., Comastri, A. *et al.* 2004, ApJ, 606, 862
11. Ptak, A., Serlemitsos, P., Yaqoob, T. *et al.* 1999, ApJS, 120, 179
12. Ranalli, P., Comastri, A., Origlia, L. *et al.* 2005, Proc. Conf. ”The X-ray universe 2005”, San Lorenzo de el Escorial, Sept. 2005, *astro-ph/0511021*
13. Read, A. & Ponman, T.2003, A&A, 409, 395
14. Smith, R., Brickhouse, N., Liedahl, D. *et al.* 2001, ApJ, 556, L91

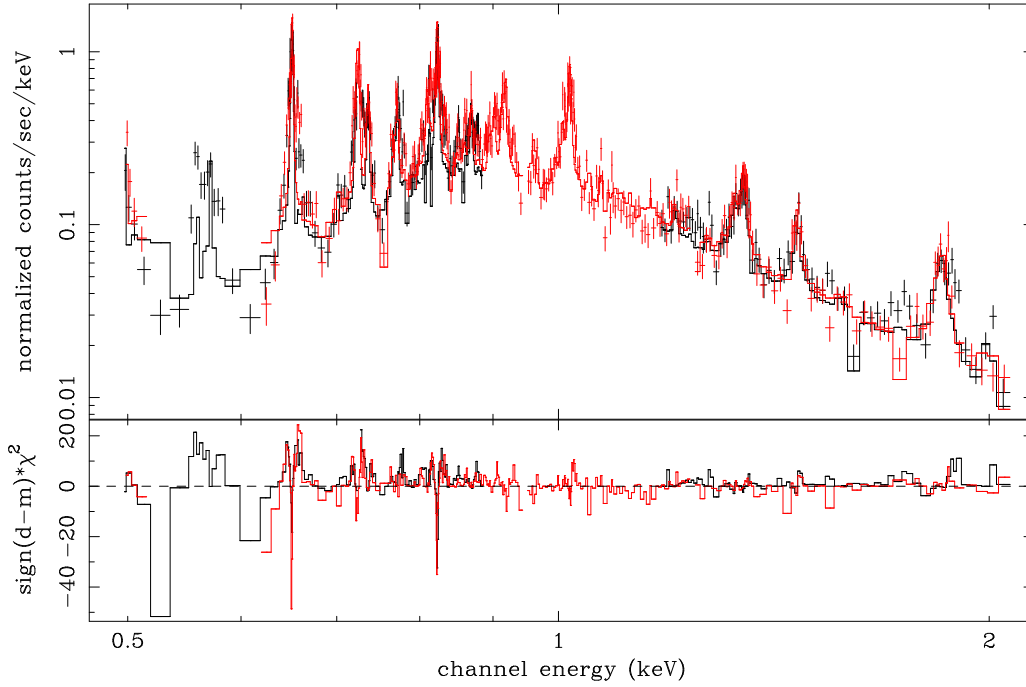


Figure 4. RGS spectrum of M82. Black, RGS1; red, RGS2. Only the first order spectra are shown for simplicity. The residuals add almost all in the O VII and O VIII lines.

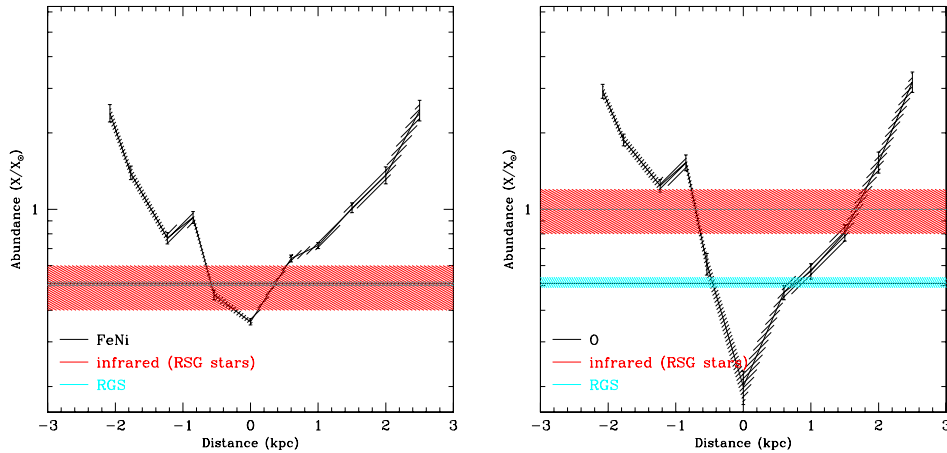


Figure 5. Variation of chemical abundances with increasing height on the galactic plane. Only O and Fe+Ni are shown for brevity. Black: abundances from X-ray MOS data. Red: abundances from infrared data (corresponding to red supergiant stars in the galaxy central region). Blue: abundances from joint EPIC-RGS fits.